Chromosoma (2008) 117:277–288
DOI 10.1007/s00412-007-0147-z

RESEARCH ARTICLE

Cytological analysis of MRE11 protein during early meiotic prophase I in Arabidopsis and tomato

Leslie D. Lohmiller · Arnaud De Muyt · Brittany Howard · Hildo H. Offenberg · Christa Heyting · Mathilde Grelon · Lorinda K. Anderson

Received: 23 July 2007 / Revised: 26 November 2007 / Accepted: 18 December 2007 / Published online: 22 February 2008

Abstract Early recombination nodules (ENs) are multiprotein complexes that are thought to be involved in synapsis and recombination, but little is known about their components or how they may be involved in these events. In this study, we describe the cytological behavior of a possible EN component, MRE11, a protein that is important for the repair of the numerous, programmed deoxyribonucleic acid double-strand breaks (DSBs) that occur early in the meiotic prophase. By immunofluorescence, many MRE11 foci were associated with chromosomal axes during early prophase I in both wild-type Arabidopsis and tomato primary microsporocytes. Similar patterns of MRE11 foci were observed in two Arabidopsis mutants (*Atspo11-1* and *Atprd1*) that are defective in DSB formation and synapsis. In tomato chromosomes, MRE11 foci were more common in distal euchromatin than in proximal heterochromatin, consistent with known EN patterns. However, electron microscopic immunogold localization demonstrated that only about 10% of ENs were labeled, and most MRE11 label was associated with synaptonemal complex components. Thus, in plants, MRE11 foci are not dependent on DSB formation, and most MRE11 foci do not correspond to ENs. More generally, our results show that the simple presence of large numbers of fluorescent foci associated with synapsing chromosomes is insufficient evidence to equate these foci with ENs.

Communicated by E.A. Nigg.

Leslie D. Lohmiller and Arnaud De Muyt contributed equally.

Electronic supplementary material The online version of this article (doi:10.1007/s00412–007–0147-z) contains supplementary material, which is available to authorized users.

L. D. Lohmiller · B. Howard
Department of Biology, Colorado State University,
Fort Collins, CO 80523, USA

A. De Muyt · M. Grelon
INRA de Versailles, Station de Génétique et d'Amélioration des Plantes UR-254, Institut Jean-Pierre Bourgin,
Route de Saint-Cyr,
78026 Versailles Cedex, France

H. H. Offenberg · C. Heyting
Molecular Genetics group, Wageningen University,
Arboretumlaan 4,
6703 BD Wageningen, The Netherlands

L. K. Anderson (✉)
Department of Biology, Program in Molecular Plant Biology,
Colorado State University,
Fort Collins, CO 80523, USA
e-mail: lorinda.anderson@colostate.edu

Introduction

In meiotic cells, numerous deoxyribonucleic acid (DNA) double-strand breaks (DSBs) are induced during prophase I as part of the normal meiotic program (Zickler and Kleckner 1999; Keeney 2001). In plants, fungi, and mammals, these DSBs and subsequently formed recombination intermediates are important for proper alignment and synapsis of homologous chromosomes, and some of the DSBs will be involved in crossing over (Zickler and Kleckner 1999; Peoples-Holst and Burgess 2005). One of the proteins that has a key role in the repair of both somatic and meiotic DSBs is MRE11 (Pâques and Haber 1999; Keeney 2001; Daoudal-Cotterell et al. 2002; D'Amours and Jackson 2002; Assenmacher and Hopfner 2004; Stracker et al. 2004; Borde 2007). MRE11 is part of a conserved multiprotein complex that includes RAD50 and XRS2 (in yeast, NBS1 in mammals). While null mutants of *MRE11* in mammals are inviable (D'Amours and Jackson 2002),

hypomorphic *mre11* mutants in mammals as well as null *mre11* mutants in budding yeast, Coprinus, worms, and plants have meiotic defects in synapsis, crossing over, and chromosome segregation (Gerecke and Zolan 2000; Keeney 2001; Chin and Villeneuve 2001; Bundock and Hooykaas 2002; Theunissen et al. 2003; Puizina et al. 2004; Cherry et al. 2007; Borde 2007). MRE11 is required for meiotic DSB formation in some but not all of these organisms (reviewed by Borde 2007). However, MRE11 is essential for later steps of meiotic recombination in all studied organisms, probably by removing SPO11 from the 5′ ends at DSB sites (Neale et al. 2005). The MRE11 complex is also proposed to play a crucial role in sensing DSBs and activating checkpoints in meiosis and in the somatic cell cycle (reviewed by Borde 2007).

Because of their role in DSB repair during meiosis, the proteins of the MRE11 complex were proposed to be components of early recombination nodules (ENs; reviewed by Anderson and Stack 2005). ENs are ellipsoidal protein complexes that are associated with synapsing chromosomes during early prophase I. During synapsis, the two axial elements (AEs) from each pair of homologous chromosomes are joined together along their entire length by transverse filaments to form the synaptonemal complex (SC, Page and Hawley 2004; de Boer and Heyting 2006). Once SCs form, AEs are called lateral elements (LEs). Because ENs are small (about 50–100 nm in their longest dimension), they are directly visible only by electron microscopy (EM). ENs are numerous and particularly common at synaptic forks where AEs are just coming together to form SC. Because of their location, frequency, and time of appearance, ENs are thought to have roles in synapsis and recombination (Zickler and Kleckner 1999; Anderson and Stack 2005), and observations that certain ENs contain RAD51 and other recombination-related proteins (DMC1, MSH4, BLM, RPA) support this hypothesis (Anderson et al. 1997; Moens et al. 2002). If ENs are involved in the early steps of recombination, then it is likely that ENs form at DSB sites, and DSB-related proteins such as MRE11 may be additional components of ENs.

MRE11 has been immunolocalized at the light microscopic (LM) level in budding yeast and mouse. While no MRE11 foci are visible in wild-type yeast cells in which DSBs appear only transiently, about 30–50 MRE11 foci per nucleus form in *rad50S* cells in which meiotic DSBs accumulate (Chua and Roeder 1998; Usui et al. 1998), consistent with an association of MRE11 in ENs. In contrast, both MRE11 and RAD50 are present at high levels in early prophase I in mouse spermatocytes, but the pattern is diffuse throughout nuclei rather than punctate (Eijpe et al. 2000b).

As part of our effort to understand the structure and function of ENs, we have examined the immunolocalization patterns of MRE11 during the early stages of prophase I in primary microsporocytes from two plants, *Arabidopsis thaliana* and tomato (*Solanum lycopersicum*). Arabidopsis allows the behavior of MRE11 protein in different mutant backgrounds to be evaluated while tomato allows higher resolution cytological analysis at both the LM and EM levels. Patterns of synapsis and the distribution of ENs have been well-studied in tomato, where ENs can be independently identified by EM based on AE/SC association, size, shape, and staining characteristics (Stack and Anderson 1986b; Anderson and Stack 2005).

In this study, we report that MRE11 forms numerous fluorescent foci, most of which are closely associated with chromosomal axes (AEs and SCs) from leptonema through early pachynema in both wild-type Arabidopsis and tomato nuclei. In Arabidopsis, *Atspo11-1* and *Atprd1* mutants do not make meiotic DSBs and homologs do not synapse. However, prophase I nuclei still possess numerous MRE11 foci in patterns similar to those observed in wild-type nuclei, demonstrating that MRE11foci are not dependent on DSB formation or synapsis. Tomato EN patterns differ from patterns of MRE11 foci because only a few ENs are present at leptonema (when the numbers of MRE11 foci are high), and no ENs are present by late pachynema (when many MRE11 foci still persist). EM immunolocalization with anti-MRE11 shows that most of the label is associated with AEs and LEs and only a small proportion (~10%) of ENs is labeled. These results show that despite some similarities between ENs and MRE11 foci in frequency and location, MRE11 is not an abundant component of most ENs in plants.

Materials and methods

Plants

Atspo11-1-1, *Atprd1-1*, and *Atmre11-3* mutants were described in Grelon et al. (2001), De Muyt et al. (2007), and Puizina et al. (2004), respectively.

Tomato (*S. lycopersicum*, formerly *Lycopersicon esculentum*, var. cherry) plants were grown from seed and maintained in a controlled temperature greenhouse. Young plants no more than 3months old were used to prepare SC spreads.

Antibody preparation

The N-terminal 430 amino acids of AtMRE11 was subcloned into the pQE31 (Qiagen) expression vector. The identification and subcloning of the N-terminal portion of the tomato SMC1 protein are described elsewhere (Lhuissier et al. 2007). Expression of the 6-His-tagged fusion proteins was induced in *E. coli* using isopropyl-β-D-thiogalactopyranoside, and the fusion proteins were purified using Ni-NTA agarose beads under denaturing conditions as described by the manufacturer (Qiagen). Polyclonal

antibodies were prepared from rabbits (MRE11) and chickens (SMC1) by Pocono Rabbit Farm and Laboratory (Pennsylvania) according to their standard protocols. Antibodies raised against this N-terminal portion of the AtMRE11 protein have been used in previous studies (Daoudal-Cotterell et al. 2002; Bundock and Hooykaas 2002). Affinity purification was done using Amino-link Columns and the Gentle Isolation Procedure (both from Pierce). Affinity-purified antibodies to MRE11 recognized only one protein band on Western blots of tomato anther proteins (see S1), although the electrophoretic mobility of the protein band was higher than expected based on the predicted molecular mass (80kDa) for AtMRE11 (Bundock and Hooykaas 2002).

SC spreads

For Arabidopsis, the preparation of prophase stage spreads for immunocytology was performed according to Armstrong et al. (2002) with the modifications described in Chelysheva et al. (2005).

For tomato, SC spreads were prepared using the technique described by Peterson et al. (1999) as modified by Chang et al. (2007). For EM, the same procedures were used except the slides had been coated with 0.6% polystrene-acrylo-nitrile (Sigma) in dichloroethane. In addition, sucrose-spread SCs from tomato were prepared using the procedure first described for lily (Anderson et al. 1994). The initial procedure was the same as described by Chang et al. (2007) except that primary microsporocytes from five tomato buds were used. After digestion, the protoplasts were treated with an equal volume of medium that contained 1% Triton X-100, and the mixture was layered onto a sucrose-step gradient composed of equal (0.4ml) volumes of 1.5 and 2.4M sucrose solutions (each containing 1% polyvinyl pyrrolidone and 0.1% Triton X-100, pH5.1) in 7 × 50-mm centrifuge tubes. The tubes were centrifuged at 10,000rpm in a swinging bucket rotor (HB-4) at 4°C in a RC2B Sorvall centrifuge for 2h. Aliquots containing SCs were placed onto agar filtration plates, picked up onto nickel grids, and immunolabeled (see below).

Immunolabeling, image preparation, and data analysis

For Arabidopsis SC spreads, ASY1 polyclonal antibodies (Armstrong et al. 2002) and affinity-purified MRE11 antibodies were used at working dilutions of 1:500 and 1:800, respectively. All observations were made using a Leica DM RXA2 microscope; photographs were taken using a CoolSNAP HQ (Roper) camera driven by Open LAB 4.0.4 software; all images were further processed with Open LAB 4.0.4 or Adobe Photoshop 8.0.

For tomato, SC spreads were immunolabeled using the procedure described by Moens et al. (2000). Each antibody incubation was performed for 1h at 37°C in a humid atmosphere. Affinity-purified anti-MRE11 antibodies were diluted 1:400 for EM and 1:800 for LM, and affinity-purified anti-SMC1 was diluted 1:25. For some preparations, we used a different rabbit anti-MRE11 antibody (affinity-purified serum from rabbit 559, diluted 1:50, prepared by Hildo Offenberg and previously reported; Daoudal-Cotterell et al. 2002; Bundock and Hooykaas 2002). Secondary antibodies, goat anti-rabbit 488 (Molecular Probes) and goat anti-chicken tetramethyl rhodamine iso-thiocyanate (Jackson), were diluted 1:500 and 1:100, respectively. In some cases, SC spreads were digested with DNaseI (Fluka, 1μg/ml in 10mM Tris buffer, pH7.5 containing 2.5mM $MgCl_2$ and 0.5 mM $CaCl_2$) at 37°C for 15min before blocking and antibody incubation. SC spreads were counterstained with 10μg/ml 4′,6-diamidino-2-phenylindole (DAPI) and mounted using Vectashield (Vector Laboratories). A Leica DM5000 B epifluorescence microscope equipped with 0-pixel-shift fluorescence cubes, a 16-bit Leica DFC 350 FX camera, and FW4000 (Leica) software were used to capture a separate fluorescent image for each probe. Grayscale images were artificially colored, and composite images were prepared using the FW4000 software before being exported for further analysis and image preparation using Adobe Photoshop 7. Any procedures used to enhance signal and decrease background were applied uniformly within each channel using the Levels command in Adobe Photoshop. For EM, immunogold labeling was done using either 6nm (1:20) or ultrasmall (1:50) gold-conjugated goat anti-rabbit secondary antibodies (Electron Microscopy Sciences) as described (Anderson et al. 1997). Ultrasmall gold particles were enhanced for 30min with silver using the instructions provided in the Aurion R-Gent SE-EM kit (Electron Microscopy Sciences). EM negatives were scanned into Adobe Photoshop 7 where they were converted into positive images, adjusted for contrast, and assembled into montages where necessary.

MRE11 foci were counted by hand (not by automatic computer software) because of variability in size and intensity of foci. Variations in numbers of MRE11 foci in the area between SC spreads were probably derived from cells that were totally disrupted by the spreading procedure because the foci were not present when only secondary antibodies were used and their frequency on different slides and in different areas of the same slide varied considerably. It is questionable whether these “background” foci would overlay SC spreads of interest, but, if they did, their low numbers (estimated to be about 30–100 per average nuclear area) and dispersed pattern would have little influence on the MRE11 focal patterns observed.

Fluorescence in situ hybridization

Tomato SC spreads that were immunolabeled with anti-SMC1 and anti-MRE11 were imaged by LM, and microscope stage coordinates were recorded so that the same SC spreads could be reimaged after fluorescence in situ hybridization (FISH). Any oil on the cover glass was removed by wiping with 100% ethanol, and the cover glass and mounting medium were removed by washing in 2× salt–sodium citrate (SSC). FISH was performed as described by Zhong et al. (1996) except that no RNase or pepsin treatments were used. The hybridization mixture (20μl per slide) included 50% formamide, 2× SSC, 10% sodium dextran sulfate, 0.25% sodium dodecyl sulfate, and 1ng biotin-labeled *A. thaliana* telomere repeat probes (Richards and Ausubel 1988). The probes were detected using fluorescein isothiocyanate (FITC)-conjugated streptavidin (Jackson) diluted 1:250, and the DNA was counterstained using 10μg/ml DAPI. For FISH, both DAPI and FITC images were captured. DAPI images were used to align the MRE11 and SMC1 immunolabeled composites with the FISH telomere repeat probes. The images were merged using Adobe Photoshop 7.0.

Results

MRE11 immunofluorescent foci during early prophase I

In Arabidopsis, immunolocalization using affinity-purified anti-MRE11 was performed together with antibodies that recognize ASY1, a meiotic protein associated with the AE of the chromosomes (Armstrong et al. 2002), to show the progress of synapsis (Fig. 1). Numerous MRE11 foci were observed from leptonema through pachynema. Many of the foci followed the chromosomal axes, particularly at leptonema–zygonema. To confirm that the signal was specific to MRE11, a similar dual immunolocalization was performed in an *Atmre11-3* mutant (Puizina et al. 2004), and no MRE11 foci were observed at any stage (Fig. 2a).

Strikingly, we could not detect any difference in MRE11 foci formation in *Atspo11-1* (Grelon et al. 2001) or *Atprd1*

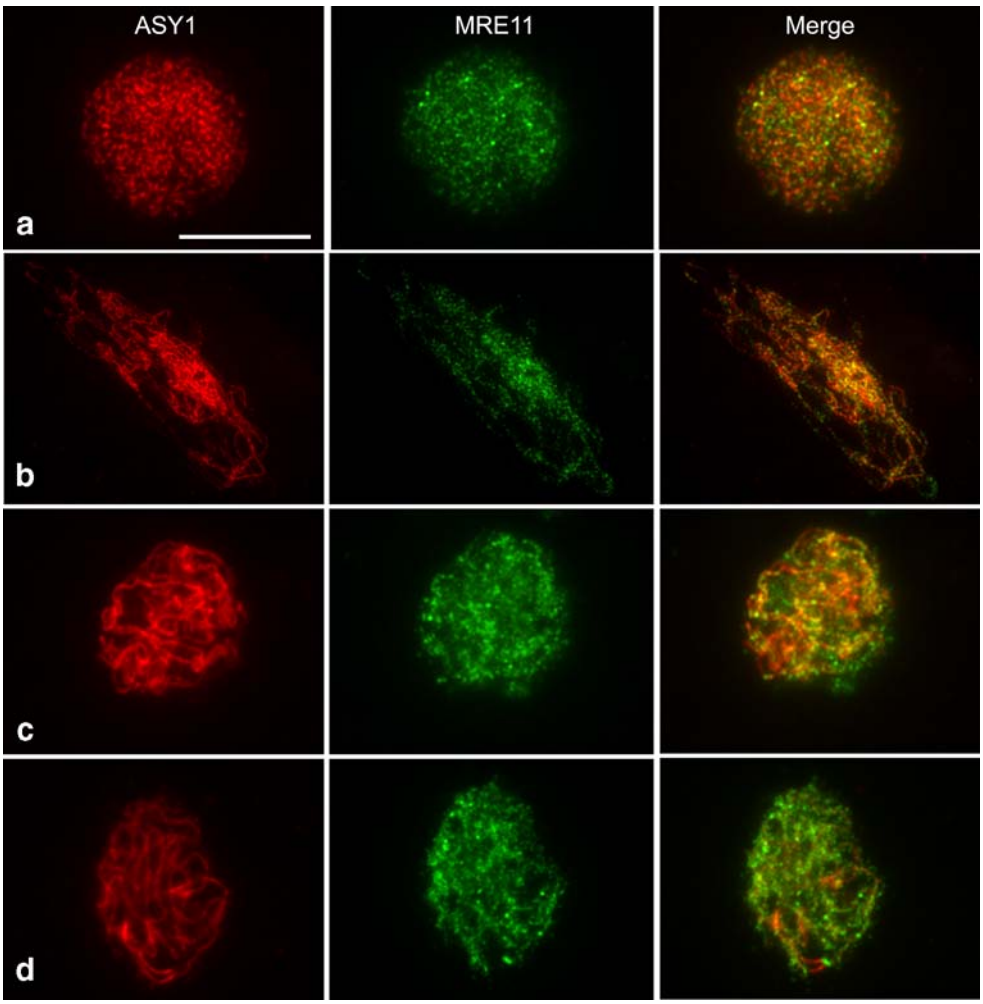

Fig. 1 Immunofluorescent localisation of ASY1 (*red*) and MRE11 (*green*) on wild-type Arabidopsis primary microsporocytes, plus the overlay of both signals (*merge*). Cells at different stage of meiosis are shown: **a** early leptonema, **b** early zygonema, **c** late zygonema **d** pachynema. *Bar* equals 10 μm

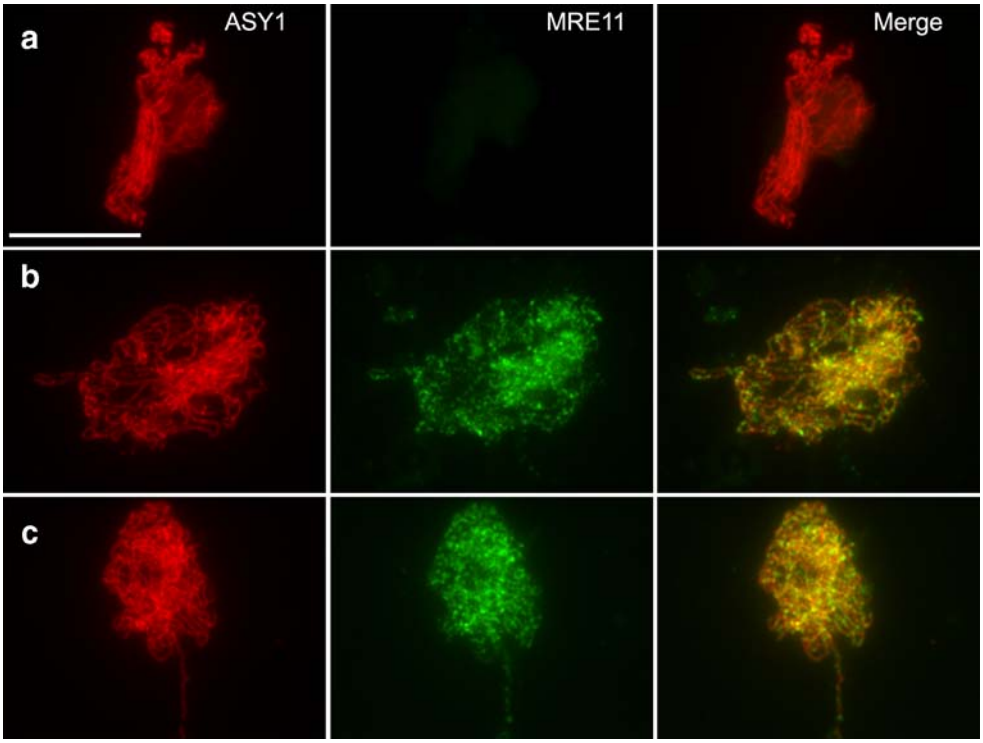

Fig. 2 Immunolocalisation of ASY1 (*red*) and MRE11 (*green*) on mutant Arabidopsis primary microsporocytes, plus the overlay of both signals (*merge*). No MRE11 signal is observed in male meiocytes from **a** *Atmre11-3* mutants, whereas MRE11 labeling is still observed on **b** *Atspo11-1-1* and **c** *Atprd1-1* mutants. *Bar* equals 10 μm

(De Muyt et al. 2007) mutants compared to the wild type (Fig. 2b and c compared to Fig. 1b), showing that numerous MRE11 foci are formed even when DSB formation and synapsis is defective.

For tomato microsporocytes, we viewed the extent of synapsis in SC spreads using affinity-purified antibodies to tomato SMC1, a sister chromatid cohesion protein that is an AE/LE component in animals and plants (Eijpe et al. 2000a; Jessberger 2002; Lam et al. 2005; Lhuissier et al. 2007). Although the SMC1 signal was rather punctuate and variable in intensity along the chromosomal axes, the signal was continuous enough to reveal each AE (or pair of LEs in SCs as brighter, thicker segments) along the length of each chromosome or bivalent, respectively (Fig. 3). There was no obvious difference in SMC1 labeling through distal euchromatin compared to proximal heterochromatin (Fig. 3e and f, S2), although such differences in SC appearance have been observed by other staining methods (Stack and Anderson 1986b; Stack et al. 1993). In addition, kinetochores did not label with anti-SMC1 (Lhuissier et al. 2007). Therefore, before immunolabeling, we examined SC spreads with phase contrast to distinguish early pachytene SCs with no kinetochores from late pachytene SCs with prominent kinetochores (Fig. 3f, S2; Stack and Anderson 1986b). This procedure did not interfere with immunolabeling because MRE11 focal patterns were the same as for slides that had not been prescanned.

Affinity-purified antibodies to MRE11 revealed numerous (>400) foci per nucleus in tomato SC spreads throughout early prophase I (Fig. 3 and Table 1). The general trend for the total number of foci per nucleus was high at leptonema (mean ≈ 760), lower from early through late zygonema (means ≈ 600 and 450, respectively) then higher again from early through late pachynema (means ≈ 700 and 1,150, respectively; Table 1). Most (>70%) of the MRE11 foci were associated with AEs and SCs at leptonema and zygonema with the remaining foci present in the surrounding chromatin (Fig. 3a–d). Early zygonema (<50% synapsis) was characterized by short stretches of SC, mostly near telomeres, which were visible as brighter and thicker segments of SMC1 label, and many MRE11 foci were associated with these distal SC segments and with AEs (Fig. 3b and c). Although each bivalent had numerous MRE11 foci, distinct regions of AEs with few foci were sometimes observed, which may correspond to heterochromatin. We did not assess how often MRE11 foci were present at or near the forks because we were unable to determine the exact location of synaptic forks because of the relatively low resolution of fluorescent images. The frequency of foci on AE segments was roughly similar at leptonema and early zygonema (0.7–1.0 foci per μm AE). By late zygonema (>50% synapsis), MRE11 foci were still common on distal, euchromatic segments, but the frequency of foci on late-synapsing AE segments, probably corresponding to heterochromatin, was only 0.20–0.37 foci per μm AE (Fig. 3d). The frequency of foci on SC segments remained relatively stable during zygonema (0.9–1.2 foci per μm SC) but at a level less than expected from doubling AE observations, *i.e.*, 1.4–2.0 foci per μm SC. At early pachynema, MRE11 foci in distal euchromatic

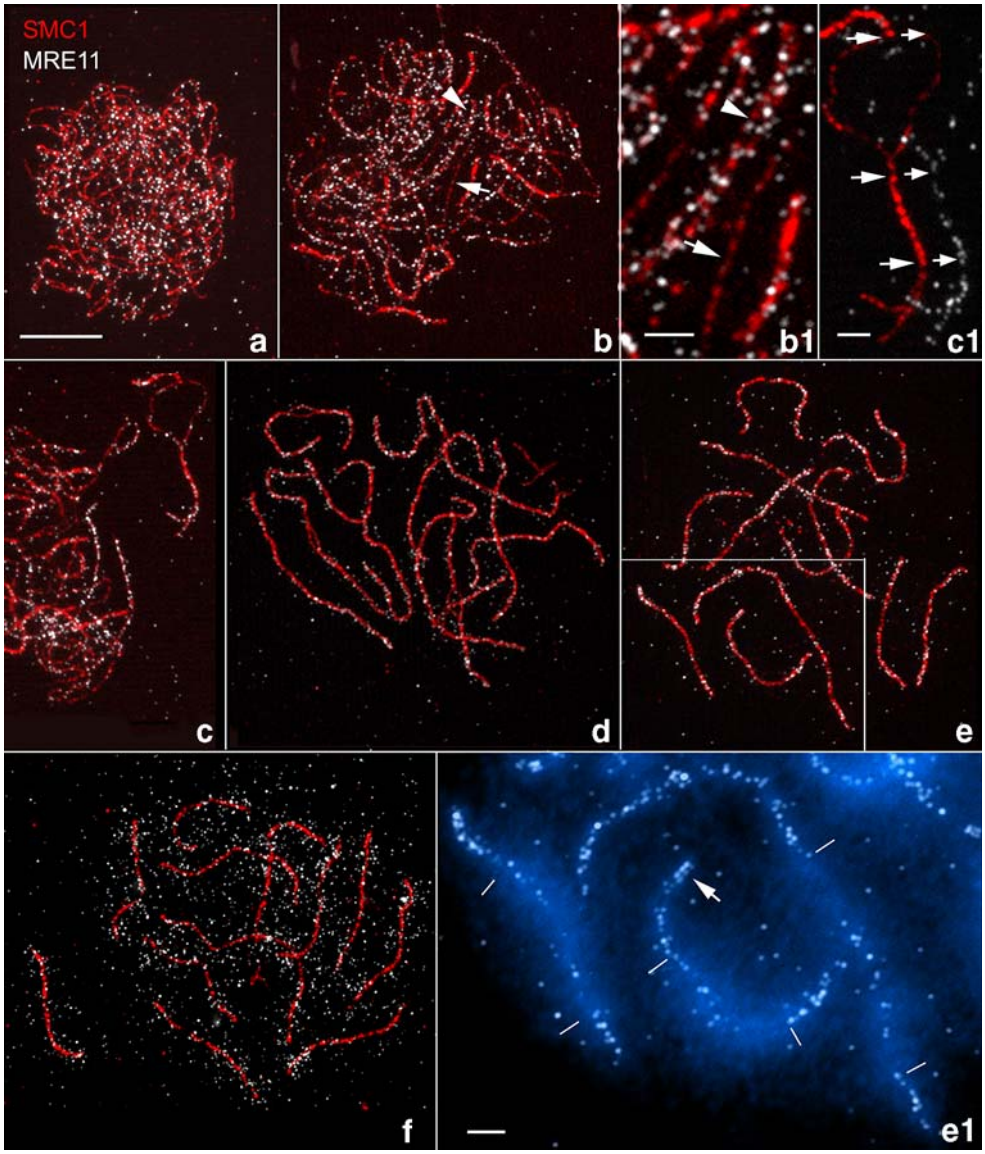

Fig. 3 Immunofluorescent localization of MRE11 (*white*) and SMC1 (*red*) on tomato SC spreads at early stages of prophase I. Numerous MRE11 foci are present at all stages, and most foci are associated with AEs and SCs until late pachynema. **a** Leptonema. **b** Early zygonema. Most AEs have many foci, and two AEs with MRE11 foci are aligned over a significant distance (*arrowhead*). Some AEs have long stretches where few foci are observed (*arrow*). A portion of this spread is shown at higher magnification in **b1**. **c** Portion of an early zygotene nucleus showing MRE11 foci of different sizes and intensities on AEs and SC segments. The SC at *upper right* has been enlarged in **c1**, and the MRE11 and SMC1 signals have been offset to make comparisons of MRE11 foci easier. The *large arrows* mark presumed synaptic forks based on the brighter SMC1 signal, and *small arrows* mark the same positions for the MRE11 channel. **d** Late zygonema. MRE11 foci are concentrated along SCs in distal euchromatin. **e** Early pachynema shows the same pattern of MRE11 foci concentrated along SCs in distal euchromatin. The *boxed area* containing three SCs from the *lower left* has been enlarged in **e1** where the DAPI and MRE11 signals have been merged. The pericentric heterochromatin in spread tomato SCs (bounded by *white bars*) forms longer loops that stain more with DAPI than distal euchromatin. In some cases, adjacent MRE11 foci have different intensities (*arrow*). Again note the concentration of MRE11 foci in euchromatin. **f** Late pachytene. SC in the *lower left* has been moved closer to the rest of the set to minimize the overall size of the figure. Many MRE11 foci are now in the surrounding chromatin. S2 shows the corresponding greyscale images for the *red* (SMC1), *white* (MRE11) and *blue* (DAPI) channels as well as the phase contrast photo of late pachytene SCs. *Bar* equals 10 μm for **a**–**f**, and 2 μm for **b1**, **c1**, and **e1**

regions were more numerous compared to foci within the pericentric heterochromatic regions of the SCs, which stain more intensely with DAPI than euchromatin (Fig. 3e). By late pachynema, a major shift in the distribution of MRE11 foci occurred, and a large proportion of foci were now observed in the chromatin surrounding the SCs (Table 1, Fig. 3f).

To confirm a change in MRE11 association from AE/SCs to chromatin, we treated tomato SC spreads with DNase I (Fig. 4 and Table 2). This step removed most of

Table 1 Frequency of MRE11 foci associated with AE and SCs at different stages of meiosis

Stage	Set number	Percent synapsis	AE length (μm)	SC length (μm)	Number foci associated with				Percent foci associated with AE/SC	Number foci per μm	
					AE	SC	Chromatin	Total		AE	SC
Leptonema	T2S4	0	806.0	0	608	0	52	660	92	0.75	–
	T3S33	0	888.0	0	761	0	94	855	89	0.86	–
	Mean	0	847.0	0	685	0	73	758	91	0.80	–
	St.Dev.	0	58.0	0	108	0	30	138	2	0.08	–
Early zygonema	T2S37	23	582.3	87.9	606	83	93	782	88	1.04	0.94
	T9S248	24	478.5	77.2	380	82	81	543	85	0.79	1.06
	T2S30	37	438	128.4	317	120	54	491	89	0.72	0.93
	Mean	28	499.6	97.8	434	95	76	605	87	0.85	0.98
	St.Dev.	8	74.4	27.0	152	22	20	155	2	0.17	0.07
Late zygonema	T4S31	62	295.4	217.8	98	249	98	445	78	0.33	1.14
	T1S35	70	204.2	235	76	279	138	493	72	0.37	1.19
	T4S52	92	49.7	290.3	10	326	68	404	83	0.20	1.12
	Mean	75	183.1	247.7	61	285	101	447	78	0.30	0.98
	St.Dev.	16	124.2	37.9	46	39	35	45	6	0.09	0.07
Early pachynema	T7S28	100	0	248.7	0	418	62	480	87	–	1.68
	T2S38	100	0	276.8	0	361	565	926	39	–	1.30
	Mean	100	0	262.8	0	390	314	703	63	–	1.49
	St.Dev.	0	0	19.9	0	40	356	315	34	–	0.27
Late Pachynema	T3S18	100	0	227.8	0	210	950	1160	18	–	0.92

the overlying chromatin allowing us to determine whether the large numbers of MRE11 foci in association with AE/SCs at earlier stages was simply due to a higher concentration of chromatin overlying these components. We found that DNase treatment did not affect the association of MRE11 foci with AE/SCs from leptotene through early pachytene (Fig. 4a–c), but the many foci present in the chromatin surrounding late pachytene SCs were largely eliminated by DNase treatment (compare Fig. 3f with Fig. 4d). To determine whether DNase treatment changed the number of MRE11 foci observed at early stages, we examined leptotene and late zygotene SC spreads from one slide, half of which had been treated with DNase I before immunolabeling, to minimize variability in number of MRE11 foci between experiments. We performed a two-way analysis of variance for total foci per nucleus to examine stage and DNase effects (Table 2). There was no interaction between stage and DNase treatment, and DNase treatment did not affect the total numbers of foci ($p>0.3$). However, stage had a major effect on total foci ($p<0.01$), with leptotene nuclei having about 30% more MRE11 foci than late zygotene nuclei.

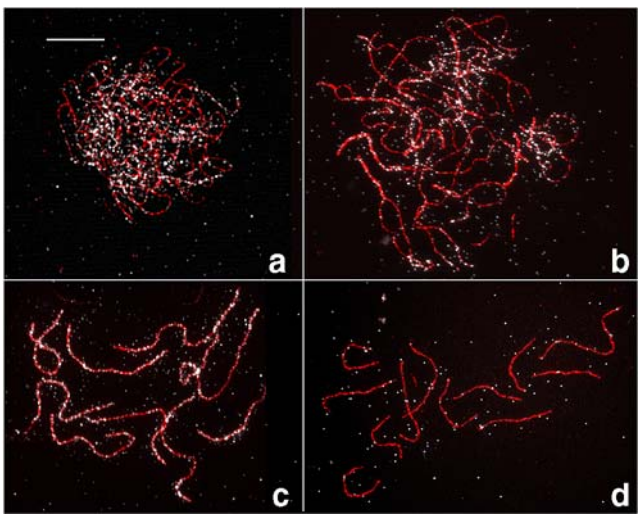

Fig. 4 Immunofluorescent localization of MRE11 (*white*) and SMC1 (*red*) on DNase I-treated SC spreads from tomato. DNase I treatment does not disrupt the association of MRE11 with AEs and SCs at **a** leptonema, **b** zygonema, or **c** early pachynema. In contrast, most MRE11 foci are removed by DNase I treatment at **d** late pachynema (compare to Fig. 3f). *Bar* equals 10 μm

In summary, MRE11 foci are present as numerous AE/LE-associated foci from leptonema to early pachynema in plants. During late pachynema, the number of MRE11 foci increases, and these foci are almost exclusively associated with chromatin. In addition, MRE11 foci are not dependent on DSB formation.

Telomere repeats and MRE11 immunolocalization in tomato

Because MRE11 has a role in telomere maintenance during development (Bundock and Hooykaas 2002), we examined whether MRE11 foci were found preferentially at telomeres

Table 2 Number of MRE11 foci per nucleus at different stages of meiosis with and without DNase I treatment, from SC spreads prepared on the same slide

Stage	DNase treatment	Number of observations	MRE11 foci per nucleus		Statistics[a]
			Mean	Standard deviation	
Leptonema	−	4	627	129	Interaction between DNase treatment and stage, F=0.00, p>0.9; DNase treatment, F=0.89, p>0.3; Stage, F=9.67, p<0.01
	+	4	578	15	
Late zygonema	−	4	458	88	
	+	4	401	158	

[a] Two-way analysis of variance

during meiosis in tomato. To distinguish telomeric ends, we performed FISH using telomeric repeats (TRs) on SC spreads that had been previously immunolabeled with SMC1 and MRE11 (Fig. 5). FISH-labeled pachytene SC spreads showed that not every end showed a detectable TR signal, probably because of the variability in number of TRs present. Nevertheless, when chromosomal ends with telomere repeats were examined at leptonema or pachynema, most did not have a distinct MRE11 signal at the tip of the SCs.

MRE11 foci and early recombination nodules in tomato

ENs are visible only by EM, so we used gold-conjugated antibodies to examine whether MRE11 is a component of ENs. Initially, we prepared spreads of SCs on plastic-coated slides using the same technique as that for fluorescent immunolocalization. Only about 11% (12 of 108) of the ENs observed were labeled with anti-MRE11. Possibly, this low labeling percentage could have been due to overlying chromatin that could interfere with penetration of the 6-nm

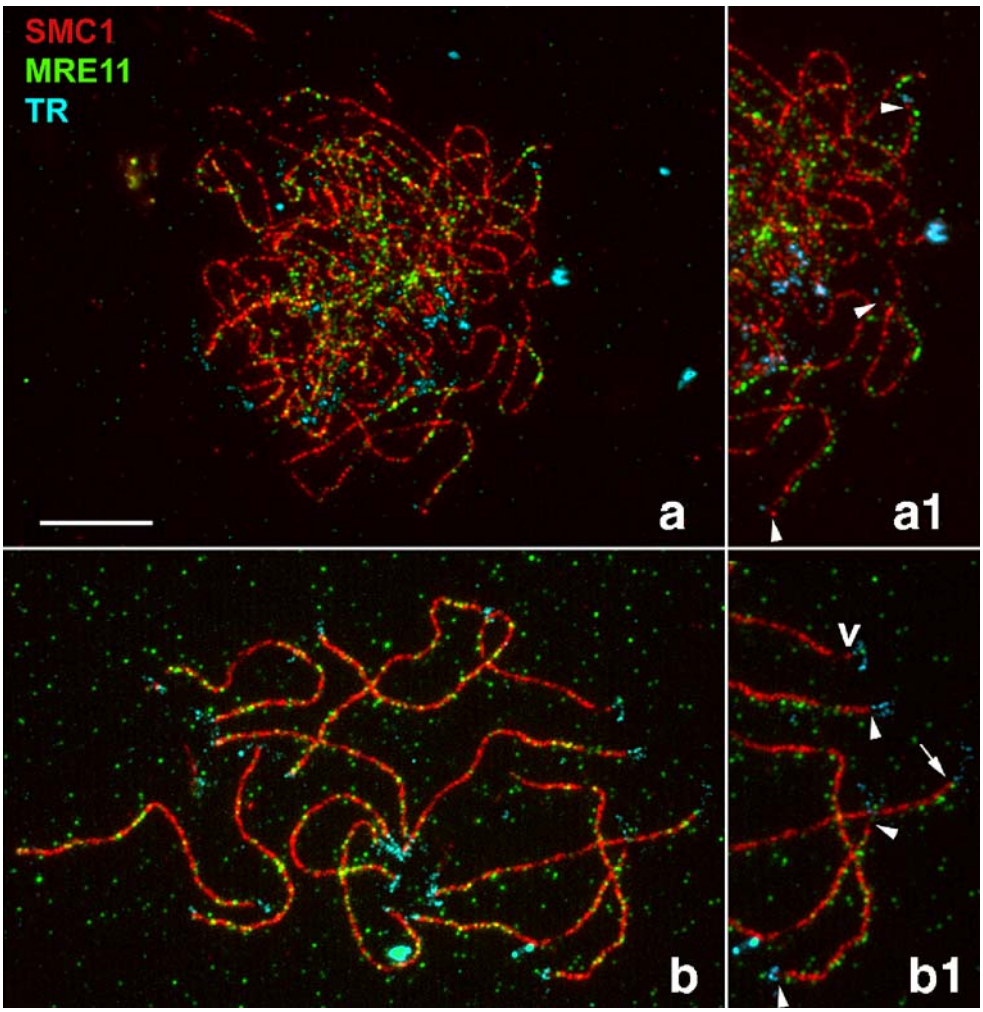

Fig. 5 Immunofluorescent localization of SMC1 (*red*) and MRE11 (*green*) followed by FISH of telomere repeats (*TR*, *blue*) at **a** leptonema and **b** pachynema. Portions of both **a** and **b** have been magnified (**a1**, **b1**) and the MRE11 signal offset from the SMC1 and telomere repeat signals to show that most apparent AE/SC ends do not have a distinct MRE11 focus (*arrowheads*), while one AE/SC end does (*arrow*). One SC has few MRE11 foci along the arm (*V*) and may be SC2 that has a heterochromatic short arm. *Bar* equals 10 μm for **a**–**b** and 12 μm for **a1** and **b1**

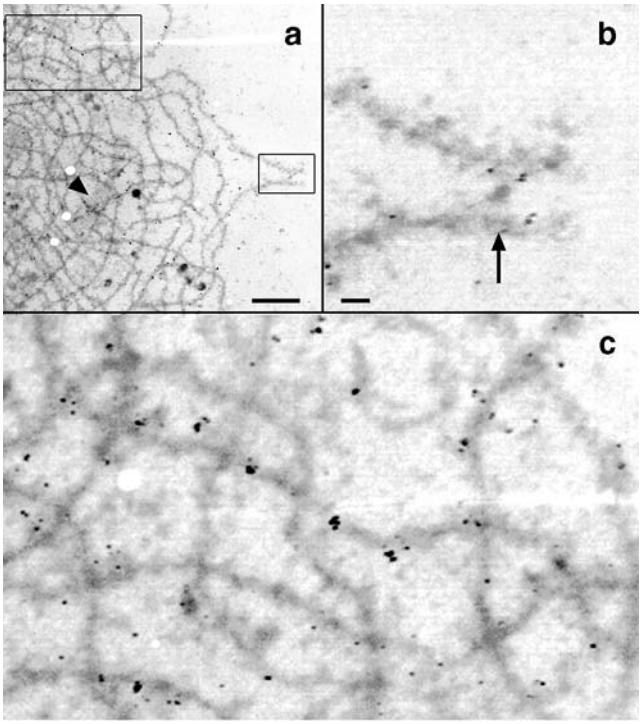

Fig. 6 Electron micrographs of DNase I-treated sucrose-spread leptotene SCs that have been immunolabeled with anti-MRE11 and silver-enhanced ultrasmall gold. **a** Lower magnification overview. A small polycomplex is present in the *lower center* of the image (*arrowhead*). *Boxed areas* are magnified in **b** and **c**. Most of the gold–silver label is associated with AEs. Although ENs are difficult to identify in these early stages, one probable EN (*arrow*) located between two AEs is not labeled, although the label is located close by the EN and near the two AEs. *Bar* equals 1 μm in **a** and 0.1 μm in **b** and **c**

gold-conjugated antibodies. Therefore, we repeated the immunolabeling using SCs that had been prepared using a sucrose step gradient (Figs. 6 and 7). The sucrose-spreading method yields many free SCs with associated ENs and LNs, which are highly accessible to antibodies (Anderson et al. 1994, 1997). We verified by immunofluorescence that the frequency and pattern of MRE11 foci associated with sucrose-spread SCs was similar to our regular SC-spreading procedure. To further reduce possible accessibility problems, we treated some of the sucrose-spread SCs with DNase I before labeling and used ultrasmall (1 nm) gold-conjugated secondary antibodies followed by silver enhancement (so that the particles can be more easily visualized) rather than 6-nm gold particles. We also increased the anti-MRE11 concentration twofold (to 1:400) because immunogold labeling is less sensitive than immunofluorescence (because the time of fluorescence exposure can be lengthened to facilitate detection). Concentrations of anti-MRE11 higher than 1:400 resulted in more background (as defined by increased gold particles on plastic surrounding SC spreads) but no additional EN labeling. After DNase digestion, labeling with anti-MRE11, and silver enhancement, many gold–silver particles were associated with AEs at leptonema (Fig. 6). Few distinct ENs could be distinguished at this time, but an EN located near the ends of two AEs at a probable synaptic initiation site was not labeled with gold–silver, although gold–silver grains were associated with both AEs near the EN. At zygonema, the gold–silver label was also associated with SCs, particularly LEs (Fig. 7). The SC-associated labeling was not due to nonspecific binding of the secondary antibodies because the number of gold–silver particles on SC segments was 6–11-fold higher (on a per area basis) for SCs labeled with anti-MRE11 compared to SCs treated with blocking solution only. Many ENs were present along SCs at zygonema, but only a few ENs were labeled (15 of 133=11%). Sometimes, the label was on the LEs immediately adjacent to the ENs (Fig. 7d), making it difficult to determine whether the label was associated with ENs or with LEs because ENs are so intimately associated with SCs and gold particles may be 14 nm away from the object labeled (7 nm each for primary and secondary antibody). Therefore, the value of 10% for labeled ENs may represent an overestimate. Assuming the label was associated with ENs, the label density (on a per area basis) for ENs was four to five times higher than for SC segments (71–144 gold particles per μm^2 for ENs compared to 17–30 gold particles per μm^2 for SC segments). Ten of 11 complete zygotene SCs had either two or three MRE11-labeled ENs.

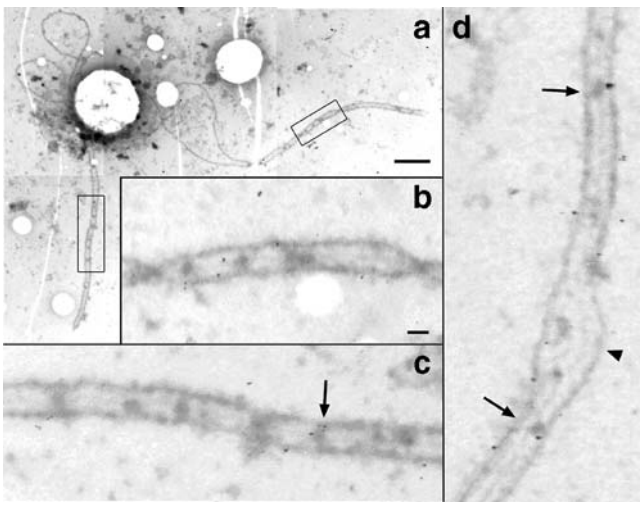

Fig. 7 Electron micrographs of DNase I-treated sucrose-spread zygotene SCs that have been immunolabeled with anti-MRE11 and silver-enhanced ultrasmall gold. **a** Lower magnification overview. *White circles* are holes in the plastic from the agar filtration plates. *Boxed areas* are magnified in **b** and **c** where several ENs are visible, but only one EN (*arrow*) is labeled with gold–silver. **d** Another late zygotene SC with a small polycomplex (*arrowhead*). Two of the ENs are labeled (*arrows*), although the label is adjacent to, not on, the ENs. Most of the gold–silver label is associated with LEs. *Bar* equals 1 μm in **a** and 0.1 μm in **b–d**

The other zygotene SC had five MRE11-labeled ENs. About the same fraction (11%) of ENs were labeled in both types of EM preparations, which indicate that the initial limited EN labeling was not due to accessibility issues. Overall, the results show that MRE11 is closely associated with AEs/LEs but MRE11 is not a major component of most ENs in plants.

Discussion

MRE11 may or may not be required for DSB formation, depending on the organism in question. However, MRE11 is essential for the subsequent repair of meiotic DSBs in all of the diverse organisms examined to date (reviewed by Borde 2007). Thus, the key role of MRE11 in the repair of meiotic DSBs is a conserved feature of meiosis. Similarly, in Arabidopsis, *AtMRE11* disruption provokes extreme chromosome fragmentation during meiosis, and the fragmentation is dependent on DSBs induced by *AtSPO11-1* (Puizina et al. 2004). However, we find that two Arabidopsis mutants that do not make meiotic DSBs, *Atspo11-1* and *Atprd1*, both have numerous MRE11 foci along chromosomal axes like those observed in wild-type Arabidopsis and tomato (Figs. 1, 2, and 3). The prevalence of AE/LE-associated MRE11 label in tomato microsporocytes suggests that MRE11 foci in *Atspo11-1* and *Atprd1* mutants are also associated with AEs. While we cannot exclude the possibility that a subset of MRE11 foci appear in response to DSB breaks (as occurs in irradiated mammalian cell lines; D'Amours and Jackson 2002), these results show that most MRE11 foci are not dependent on the creation of meiotic DSBs. Such observations are consistent with other studies showing that MRE11 can load onto chromatin before DSB formation (Ohta et al. 1998; Mirzoeva and Petrini 2003; Borde et al. 2004). Our results also suggest that MRE11 in plants has meiotic functions in addition to processing SPO11-dependent DSBs. Although there is no clear consensus on what such functions might be, one possibility is that MRE11 is part of a DNA damage-sensing complex (Mirzoeva and Petrini 2003) that is present throughout meiosis, even in the absence of meiosis-specific DSBs. Another possibility is that the close association between MRE11 and SC components in plants is related to proposed monitoring and coordinating functions that link recombination progression and meiotic chromosome behavior (Kleckner 2006). MRE11 may also participate in chromatin organization by preparing chromatin for DSB formation (Eijpe et al. 2000b; Borde et al. 2004; although this function is not required for DSB formation in Arabidopsis; Puizina et al. 2004) and/or by effecting chromatin condensation (Gerecke and Zolan 2000). Analysis of mutations less severe than the currently available null mutations may help to resolve whether MRE11 has any of these roles in plants.

Although MRE11 has been reported to have a role in telomere maintenance during somatic development in Arabidopsis (Bundock and Hooykaas 2002), we did not regularly observe MRE11 foci at telomeres of AEs/SCs from leptonema through pachynema (Fig. 5). While it is possible that MRE11 is not important for telomere maintenance during prophase I in tomato primary spermatocytes, there are other possibilities: (1) only a few MRE11 molecules (and not enough to yield a distinct focus) are involved at this time, (2) the process does not all happen at the same time, and/or (3) telomerase activity during meiosis (McKnight et al. 2002; Riha et al. 2006) minimizes the role of MRE11.

MRE11 was considered to be a likely EN component based on its role in DSB repair (Puizina et al. 2004; Anderson and Stack 2005), and, although our conclusions do not support this claim, some of our results are consistent with this suggestion. For example, like ENs, MRE11 foci are distinct and closely associated with AEs and SCs from leptonema through early pachynema in both wild-type tomato and Arabidopsis (Figs. 1 and 3). In tomato, the MRE11 foci are located primarily but not exclusively in the distal euchromatic segments of the chromosomes, and up to late pachynema, their association with the SC is stable even after DNase treatment (Fig. 4; Moens et al. 1987, 2002; Anderson et al. 1997, 2001). As pachynema proceeds, the proportion of MRE11 foci associated with chromatin increases, again consistent with the abrupt loss of ENs from SCs during early pachynema (Stack and Anderson 1986a; Anderson and Stack 2005). Finally, some tomato ENs contain MRE11 as determined by immunogold localization (Fig. 7). However, in Arabidopsis, the number of MRE11 foci exceeds the expected number of ENs (as estimated by Dmc1 foci, Chelysheva et al. 2007), and in tomato, immunogold localization revealed that most of the gold label at all early prophase I stages is associated with AE/LEs, not ENs. Only about 10% of ENs label with gold regardless of whether the preparations are treated with DNase I, prepared using sucrose step gradients, or labeled with ultrasmall gold-conjugated antibodies, all procedures that should increase antibody access to ENs. This low level of label is much below what would be expected if ENs beneath the SC were inaccessible to antibodies because this would only affect about half of the visible ENs. It is possible that the amount of MRE11 in some (or many) ENs was too low to detect by immunogold methods. However, we did not obtain more EN labeling with increased concentrations of anti-MRE11, and the level of immunogold label on SCs (estimated to be around 1–2 "foci" per μm SC) was roughly similar to our LM observations of MRE11 foci. Even if immunogold labeling was not

sensitive enough to label all ENs that contained Mre11, several other results also indicate that most MRE11 foci do not correspond to ENs. For example, large numbers (~600–800 per nucleus) of MRE11 foci are associated with AEs at leptonema, but only a few (<50 per nucleus) ENs have been observed in leptotene nuclei in tomato (Fig. 6; Stack and Anderson 1986b). Similarly, there are about three times more MRE11 foci than ENs per μm of euchromatic AE length during early zygonema (~0.8 MRE11 foci vs 0.27 ENs per μm AE; Table 1; Anderson et al. 2001). It is unlikely that the turnover of MRE11 in ENs is involved in the discrepancy because low frequencies of labeled ENs were observed as early as leptonema and throughout zygonema when high numbers of MRE11 foci were observed. Thus, patterns of MRE11 foci during early prophase I superficially resemble patterns of ENs, but closer analysis shows that most MRE11 foci do not directly correspond to ENs or to DSB sites. More generally, these results indicate that the mere appearance of fluorescent foci in association with AEs and SCs during synapsis is insufficient to equate foci with ENs.

While most MRE11 foci do not correspond to ENs, the label we observed associated with ENs does appear to be specific (four to five times above that associated with SCs). In addition, of the 11 complete zygotene SCs for which EN labeling was quantified, all but one SC (with five labeled ENs) had two or three labeled ENs. This suggests the intriguing but clearly speculative possibility that these few ENs may be the ones involved in formation of crossovers. Additional work with other antibodies may help to determine whether this is the case.

Acknowledgments We thank Song-Bin Chang for providing biotin-labeled telomere repeat probes for FISH and Edu Holub and the animal facilities group at Wageningen University for expert technical assistance. We also thank Stephen Stack and two anonymous reviewers for valuable comments on the manuscript. This research was supported by a grant from the National Science Foundation (MCB-064344 to LKA).

References

Anderson LK, Stack SM (2005) Recombination nodules in plants. Cytogenet Genome Res 109:198–204

Anderson LK, Stack SM, Todd RJ, Ellis RP (1994) A monoclonal antibody to lateral element proteins in synaptonemal complexes of *Lilium longiflorum*. Chromosoma 103:357–367

Anderson LK, Offenberg HH, Verkuijlen WMHC, Heyting C (1997) RecA-like proteins are components of early meiotic nodules in lily. Proc Natl Acad Sci USA 94:6868–6873

Anderson LK, Hooker KD, Stack SM (2001) The distribution of early recombination nodules on zygotene bivalents from plants. Genetics 159:1259–1269

Armstrong SJ, Caryl AP, Jones GH, Franklin FCH (2002) Asy1, a protein required for meiotic chromosome synapsis, localizes to axis-associated chromatin in *Arabidopsis* and *Brassica*. J Cell Sci 115:3645–3655

Assenmacher N, Hopfner K-P (2004) MRE11/RAD50/NBS1: complex activities. Chromosoma 113:157–166

Borde V (2007) The multiple roles of the Mre11 complex for meiotic recombination. Chrom Res 15:551–563

Borde V, Lin W, Novikov E, Petrini JH, Lichten M, Nicolas A (2004) Association of Mre11p with double-strand break sites during yeast meiosis. Mol Cell 13:389–401

Bundock P, Hooykaas P (2002) Severe developmental defects, hypersensitivity to DNA-damaging agents, and lengthened telomeres in Arabidopsis MRE11 mutants. Plant Cell 14:2451–2462

Chang S-B, Anderson LK, Sherman JD, Royer SM, Stack SM (2007) Predicting and testing physical locations of genetically mapped loci on tomato pachytene chromosome 1. Genetics 176:2131–2138

Chelysheva L, Diallo S, Vezon D, Gendrot G, Vrielynck N, Belcram K, Rocques N, Marquez-Lema A, Bhatt AM, Horlow C, Mercier R, Mezard C, Grelon M (2005) AtREC8 and AtSCC3 are essential to the monopolar orientation of the kinetochores during meiosis. J Cell Sci 118:4621–4632

Chelysheva L, Gendrot G, Vezon D, Doutriaux M-P, Mercier R, Grelon M (2007) Zip4/Spo22 is required for class I CO formation but not for synapsis completion in *Arabidopsis thaliana*. PLoS Genet 3:0802–0813

Cherry SM, Adelman CA, Theunissen JW, Hassold TJ, Hunt PA, Petrini JHJ (2007) The Mre11 complex influences DNA repair, synapsis, and crossing over in murine meiosis. Curr Biol 17:373–378

Chin GM, Villeneuve AM (2001) C. elegans mre-11 is required for meiotic recombination and DNA repair but is dispensable for the meiotic G2 DNA damage checkpoint. Genes Devel 15:522–534

Chua PR, Roeder GS (1998) Zip2, a meiosis-specific protein required for the initiation of chromosome synapsis. Cell 93:349–359

D'Amours D, Jackson SP (2002) The Mre11 complex: at the crossroads of DNA repair and checkpoint signalling. Nat Rev Mole Cell Biol 3:317–327

Daoudal-Cotterell S, Gallego ME, White CI (2002) The plant Rad50-Mre11 protein complex. FEBS Lett 516:164–166

de Boer E, Heyting C (2006) The diverse roles of transverse filaments of synaptonemal complexes in meiosis. Chromosoma 115:220–234

De Muyt A, Vezon D, Gendrot G, Gallois J-L, Stevens R, Grelon M (2007) AtRPD1 is required for meiotic double-strand break formation in Arabidopsis thaliana. EMBO J 26:4126–4137

Eijpe M, Heyting C, Gross B, Jessberger R (2000a) Association of mammalian SMC1 and SMC3 proteins with meiotic chromosomes and synaptonemal complexes. J Cell Sci 113:673–682

Eijpe M, Offenberg HH, Goedecke W, Heyting C (2000b) Localisation of RAD50 and MRE11 in spermatocyte nuclei of mouse and rat. Chromosoma 109:123–132

Gerecke EE, Zolan ME (2000) An mre11 mutant of Coprinus cinereus has defects in meiotic chromosome pairing, condensation and synapsis. Genetics 154:1125–1129

Grelon M, Vezon D, Gendrot G, Pelletier G (2001) AtSPO11-1 is necessary for efficient meiotic recombination in plants. EMBO J 20:589–600

Jessberger R (2002) The many functions of SMC proteins in chromosome dynamics. Nat Rev Mol Cell Biol 3:767–778

Keeney S (2001) Mechanism and control of meiotic recombination initiation. Curr Top Dev Biol 52:1–53

Kleckner N (2006) Chiasma formation: chromatin/axis interplay and the role(s) of the synaptonemal complex. Chromosoma 115:175–194

Lam WS, Yang X, Makaroff CA (2005) Characterization of *Arabidopsis thaliana* SMC1 and SMC3: evidence that AtSMC3 may function beyond chromosome cohesion. J Cell Sci 118:3037–3048

Lhuissier FGP, Offenberg HH, Wittich PE, Vischer NOE, Heyting C (2007) The mismatch repair protein MLH1 marks a subset of strongly interfering crossovers in tomato. Plant Cell 19:862–876

McKnight TD, Riha K, Shippen DE (2002) Telomeres, telomerase, and stability of the plant genome. Plant Mol Biol 48:331–337

Mirzoeva OK, Petrini JHJ (2003) DNA replication-dependent nuclear dynamics of the Mre11 complex. Mol Cancer Res 1:207–218

Moens PB, Heyting C, Dietrich AJJ, van Raamsdonk W, Chen Q (1987) Synaptonemal complex antigen location and conservation. J Cell Biol 105:93–103

Moens PB, Freire R, Tarsounas M, Spyropoulos B, Jackson SP (2000) Expression and nuclear localization of BLM, a chromosome stability protein mutated in Bloom's syndrome, suggest a role in recombination during meiotic prophase. J Cell Sci 113:663–672

Moens PB, Kolas NK, Tarsounas M, Marcon E, Cohen PE, Spyropoulos B (2002) The time course and chromosomal localization of recombination-related proteins at meiosis in the mouse are compatible with models that can resolve the early DNA–DNA interactions without reciprocal recombination. J Cell Sci 115:1611–1622

Neale MJ, Pan J, Keeney S (2005) Endonucleolytic processing of covalent protein-linked DNA double-strand breaks. Nature 436:1053–1057

Ohta K, Nicolas A, Furuse M, Nabetani A, Ogawa H, Shibata T (1998) Mutations in the MRE11, RAD50, XRS2, and MRE2 genes alter chromatin configuration at meiotic DNA double-stranded break sites in premeiotic and meiotic cells. Proc Natl Acad Sci USA 95:646–651

Page SL, Hawley RS (2004) The genetics and molecular biology of the synaptonemal complex. Annu Rev Cell Dev Biol 20:525–558

Pâques F, Haber JE (1999) Multiple pathways of recombination induced by double-strand breaks in Saccharomyces cerevisiae. Microbiol Mol Biol Rev 63:349–404

Peoples-Holst TL, Burgess SM (2005) Multiple branches of the meiotic recombination pathway contribute independently to homolog pairing and stable juxtaposition during meiosis in budding yeast. Genes Devel 19:863–874

Peterson DG, Lapitan N, Stack SM (1999) Localization of single- and low-copy sequences on tomato synaptonemal complex spreads using fluorescence in situ hybridization (FISH). Genetics 152:427–439

Puizina J, Siroky J, Mokros P, Schweizer D, Riha K (2004) Mre11 deficiency in Arabidopsis is associated with chromosomal instability in somatic cells and Spo11-dependent genome fragmentation during meiosis. Plant Cell 16:1968–1978

Richards EJ, Ausubel FM (1988) Isolation of a higher eukaryotic telomere from *Arabidopsis thaliana*. Cell 53:127–136

Riha K, Heacock ML, Shippen DE (2006) The role of the nonhomologous end-joining DNA double-strand break repair pathway in telomere biology. Ann Rev Genet 40:237–277

Stack S, Anderson L (1986a) Two-dimensional spreads of synaptonemal complexes from solanaceous plants. III. Recombination nodules and crossing over in *Lycopersicon esculentum* (tomato). Chromosoma 94:253–258

Stack SM, Anderson LK (1986b) Two-dimensional spreads of synaptonemal complexes from solanaceous plants. II. Synapsis in *Lycopersicon esculentum*. Am J Bot 73:264–281

Stack SM, Sherman JD, Anderson LK, Herickhoff LS (1993) Meiotic nodules in vascular plants. In: Sumner AT, Chandley AC (eds) Chromosomes today. Chapman & Hall, London, pp 301–311

Stracker TH, Theunissen J-WF, Morales M, Petrini JHJ (2004) The Mre11 complex and the metabolism of chromosome breaks: the importance of communicating and holding things together. DNA Repair 3:845–854

Theunissen JW, Kaplan MI, Hunt PA, Williams BR, Ferguson DO, Alt FW, Petrini JHJ (2003) Checkpoint failure and chromosomal instability without lymphomagenesis in Mre11ATLD1/ATLD1 mice. Mol Cell 12:1511–1523

Usui T, Ohta T, Oshiumi H, Tomizawa J, Ogawa H, Ogawa T (1998) Complex formation and functional versatility of Mre11 of budding yeast in recombination. Cell 95:705–716

Zhong X-B, de Jong JH, Zabel P (1996) Preparation of tomato meiotic pachytene and mitotic metaphase chromosomes suitable for fluorescence in situ hybridization (FISH). Chromosome Res 4:24–28

Zickler D, Kleckner N (1999) Meiotic chromosomes: Integrating structure and function. Ann Rev Genet 33:603–754